MODELING AND IDENTIFICATION OF THE SOURCE OF OSCILLATIONS IN WEB TENSION

By

C. Branca, P.R. Pagilla, and K. N. Reid
Oklahoma State University
USA

ABSTRACT

Although there has been much work in dynamic modeling of different web handling elements and web longitudinal behavior, efforts to systematically validate models by experimentation on a web platform are non-existent. Existing literature has extensively used dynamic models for numerical analysis and/or design of control systems without adequate experimental validation of the models. One of the well-known modeling techniques for creating a model for the entire web line is based on the concept of primitive elements. In this approach every primitive element of the web line is modeled separately using first principles approach, and then the entire web line model is obtained by appropriately combining the primitive element models. The goal of this paper is to present results from recent investigations on validation of key primitive element models. Model refinement and modifications are also considered when sufficient level of agreement between model and experimental data was not obtained.

Since the dynamic model for web tension in a span is nonlinear, designing experiments for web line model validation is a formidable task. There are a few known model validation techniques for nonlinear systems but these do not provide any clear procedures that can be applied to the web line. Therefore, the approach taken in this study was to consider test cases of experimentation thatmimic typical web line operations in the industry such as acceleration/deceleration of the line and running the line at a constant speed. A number of test cases for model simulations and experimentation were considered. A representative sample of the results is shown and discussed.

Data from the simulations of existing models did not contain the oscillations found in measured tension signals. This study also considered refinement and modifications of dynamicmodels that would lead to better agreement between the model and experimental data. It was found that span length variations introduced by out-of-round and/or eccentric rollers are the direct cause of oscillations in the tension signal. A refined model for web tension that includes span length variations is given. Comparison of the data from

simulations of the refined model and experimental data shows a high level of agreement. These results are shown and discussed.

NOMENCLATURE

A	area of cross section of the web [in^2]
B	viscous damping coefficient [lbf sec/rad]
E	modulus of elasticity (Young's modulus) $\left[\frac{lbf}{in^2}\right]$
f	Fourier series fundamental frequency [Hz]
J	moment of inertia [lb ft^2]
K_p	proportional gain in a PI controller
K_{ref}	reference proportional gain
L	free span web length [m]
m	mass [lb]
R	radius of the roller [m]
t	thickness [in]
T	web tension [lbf]
v	web speed on roller [ft/min]
w	web width [in]
ε	web strain
ρ	web density $\frac{lb}{ft^3}$
τ	driving torque [lbf]
ζ	damping ratio for a second order system
ω	roller angular velocity [rad/sec]

Subscripts

i	span or roller number
n	pertaining to unstretched web
r	pertaining to rewind or winder
u	pertaining to unwind
w	pertaining to the web

INTRODUCTION

Web lines can differ widely, either because of their layout or because of the kind of components that compose the line. In order to come up with a systematic approach to modeling of web lines, it is necessary to approach the problem in a modular way. The concept of primitive elements is introduced for this reason. It is possible to consider a set of elementary components which form the building blocks for every possible web line. Modeling the primitive elements is easier than the entire line. The primitive element models are developed from the application of first principles. Once the models for the primitive elements are developed, the model of any web line can be obtained by composing the models of primitive elements by considering the layout of the line.

One can ask several fundamental questions during the process of model validation: How good are the primitive element models derived using the first principles? How well does the simulated data correlate with the experimental data? If the model simulated data does not follow the experimental data, is it due to first order effects (the model derived from the first principles is incorrect) or due to second order effects (some non-ideal

effects in the process are not included in the model)? To answer these questions, a model of a web line (called the Euclid Web Line (EWL)) was developed using available models for the primitive elements and the output data from the simulations was compared with the experimental data collected on the real machine. Several experiments and simulations were conducted, with both stationary and moving web. The outcome of this first set of experiments is that the first principles based models are able to predict the behavior of the tension in an average sense, but they were not able to reproduce tension oscillations which are seen in the experimental data.

The fact that the macroscopic response of tension was reproduced in the model data led to believe that first order effects are included in the model. Therefore, the reason for the mismatch must be due to some second order effects. In deriving the dynamic equations for the primitive elements, it was assumed that they exhibit ideal behavior. In real situations many primitive elements are not ideal, and hence, their non-ideal characteristics will affect tension response. Therefore, non-ideal effects must be systematically included in the models since it is unclear which non-ideal effects are causing discrepancies between model and experimental data. Further, once it is known that a non-ideal component is causing these tension oscillations, a modeling mechanism must be determined to appropriately include that particular non-ideal effect into the model. One of the objectives was to study the non-ideal components and include their effects into the web line model and verify whether their inclusion makes the data from model simulations correlate closely with the experimental data.

It is well known that the presence of play between moving parts (backlash) will deteriorate system performance by inducing oscillations, limit cycles and even instability. Backlash is commonly found in mechanical transmission between motor and roll shaft. In addition to backlash, compliance of shafts/belts will also reduce performance. These two effects were incorporated into the web line models and simulations were conducted with different values of backlash and compliance. Comparison of simulation and experimental data showed that the inclusion of these non-ideal effect did not adequately capture the tension oscillations in the measured data.

It is also known that non-ideal components such as out-of-round material rolls and eccentric rollers induce tension disturbances. One of the objectives was to find a mechanism through which the model can be refined to include these non-ideal effects. It was determined that span length variations introduced by out-of-round and eccentric rollers cause these oscillations in the tension signal. The span tension model is appropriately modified to include span length variations.

Model analysis and experimentation has revealed that every non-ideal rotating element, either because of eccentricity or out-of-roundness, will introduce tension oscillations which are integer multiple of a fundamental frequency f, a frequency that can be computed by knowing the radius of the rotating element and the line speed. Using this fundamental frequency in the computation of the span length variations, the refined tension model is able to capture almost all of the frequency content found in the measured tension signal.

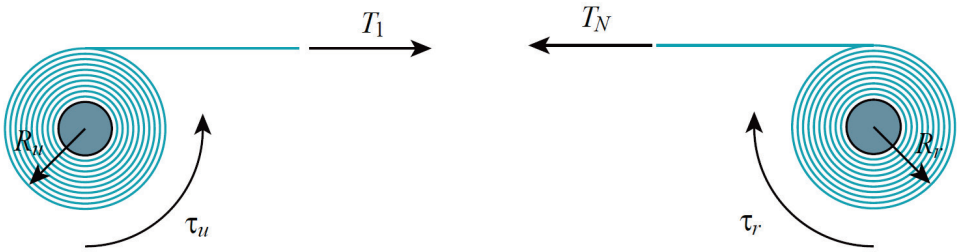

Figure 1 – Unwind and rewind.

The remainder of the paper is organized as follows: Section 2 will introduce dynamic models for the primitive elements. Section 3 will give a literature review on nonlinear system identification and model validation. Section 4 describes experimental model validation and proposed model modifications considered to match the data from model simulations and experimental data from the web line. Section 5 gives conclusions and suggestions for future work.

PRIMITIVE ELEMENTS MODELS

Material Roll Models

A schematic of the unwind roll is shown in Fig. 1(a). The dynamic equation that describes the motion of the unwind roll is given by [1]:

$$\frac{d}{dt}\left(J_u(t)\omega_u(t)\right) = -b\omega_u(t) + R_u(t)T_1(t) - \tau_u \qquad \{1\}$$

where $J_u(t)$ is the inertia of the roll, $\omega_u(t)$ is the angular velocity, b is the viscous friction coefficient, $R_u(t)$ is the radius of the roll, $T_1(t)$ is web tension, and τ_u is the torque transmitted from the motor to the roll through a coupling. Note that all the variables refer to the roll side. Expanding {1}:

$$J_u\dot{\omega}_u = -b\omega_u + R_u T_1 - \tau_u - \dot{J}_u\omega_u \qquad \{2\}$$

The moment of inertia J_u is given by:

$$J_u(t) = J_0 + J_w(t) \qquad \{3\}$$

where J_0 is the inertia of the core shaft, core, coupling, and motor, and J_w is the inertia of the web material, which is time-varying as the web is unwound. The moment of inertia J_w can be written as a function of the radius:

$$J_w = \frac{m_w}{2}(R^2 + R_c^2) = \frac{\pi}{2}\rho_w w_w (R^2 - R_c^2)(R^2 + R_c^2) = \frac{\pi}{2}\rho_w w_w (R^4 - R_c^4) \qquad \{4\}$$

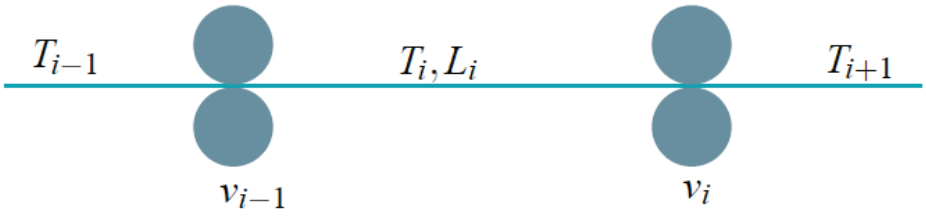

Figure 2 – Web Span

where m_w is the mass of the web, R_c is the radius of the core of the roller, ρ_w is the density of the web and w_w is its width. The external radius of the roll is also a function of time, as the web leaves the roll the radius decreases. In particular, the radius decreases by $\Delta R_u = t_w$, with t_w being the web thickness, every one revolution of the roll. The time that the roll takes to rotate 2π radians is $\Delta t = 2\pi/\omega_u$. Therefore, the dynamic equation for the roll radius can be expressed as

$$\dot{R}_u = \lim_{\Delta t \to 0} \frac{\Delta R_u}{\Delta t} = -\frac{t_w \omega_u}{2\pi} \qquad \{5\}$$

From {1} and {5} $\dot{J}_u$ is given by

$$\dot{J}_u = 2\pi\rho_w w_w R_u^3 \dot{R}_u = -\rho_w w_w R_u^3 t_w \omega_u \qquad \{6\}$$

Hence, the dynamic equation for the angular velocity of the unwind roll is

$$J_u \dot{\omega}_u = -b_u \omega_u + R_u T_1 - \tau_u + \rho_w w_w R_u^3 t_w \omega_u^2 \qquad \{7\}$$

For the rewind roll model an analogous discussion can be made, the only difference is that the radius will be increasing and the tension of the web will be pulling the roller in opposition to the sense of rotation of the roller (see Fig. 1(b)). Therefore, the dynamic equation for the rewind roll will be:

$$J_r \dot{\omega}_r = -b\omega_r - R_r T_n + \tau_r - \rho_w w_w R_r^3 t_w \omega_r^2 \qquad \{8\}$$

Web Span Model

Modeling of tension in a web span has been addressed in several studies, examples are [2, 3], the fundamental idea behind the derivation of the dynamic equation is the conservation of mass in the control volume encompassing a web span between two rollers, which is: at any moment, the variation of the mass of web in the span is equal to the difference between the amount of mass coming from the previous span and the mass leaving the span to enter the next span. For a web span between two rollers (see Fig. 2) mass conservation can be written as

$$\frac{d}{dt} \int_{x_{i-1}(t)}^{x_i(t)} \rho(x,t) A(x,t) dx = \rho_{i-1} A_{i-1} v_{i-1} - \rho_i A_i v_i \qquad \{9\}$$

where, $x_{i-1}(t)$ and $x_i(t)$ are the positions of the $(i-1)$-th and i-th roller, ρ is the density

of the web, A is the cross sectional area, and v is the velocity of the web. Now the mass of an infinitesimal element of web in the transport direction is given by

$$dm = \rho dx w h = \rho dx A = \rho_n dx_n w_n h_n = \rho_n A_n dx_n \quad \{10\}$$

where the subscript n denotes the unstretched state. Considering the relation between stretched and unstretched material:

$$dx = (1 + \varepsilon_x) dx_n \quad \{11\}$$

it is possible to write:

$$\frac{\rho(x,t)A(x,t)}{\rho_n(x,t)A_n(x,t)} = \frac{dx_n}{dx} = \frac{1}{1+\varepsilon_x(x,t)} \quad \{12\}$$

which can be rearranged as:

$$\rho(x,t)A(x,t) = \frac{\rho_n(x,t)A_n(x,t)}{1+\varepsilon_x(x,t)} \quad \{13\}$$

Substitution of {13} in {9} gives

$$\frac{d}{dt}\int_{x_{i-1}(t)}^{x_i(t)} \frac{\rho_n(x,t)A_n(x,t)}{1+\varepsilon_x(x,t)} dx = \frac{\rho_{n_{i-1}}(x,t)A_{n_{i-1}}(x,t)v_{i-1}}{1+\varepsilon_{x_{i-1}}(x,t)} - \frac{\rho_{n_i}(x,t)A_{n_i}(x,t)v_i}{1+\varepsilon_{x_i}(x,t)} \quad \{14\}$$

Under the assumption that the cross sectional area A and the density ρ of the unstretched material is constant, {14} can be simplified to the following:

$$\frac{d}{dt}\int_{x_{i-1}(t)}^{x_i(t)} \frac{1}{1+\varepsilon_x(x,t)} dx = \frac{v_{i-1}}{1+\varepsilon_{x_{i-1}}(x,t)} - \frac{v_i}{1+\varepsilon_{x_i}(x,t)} \quad \{15\}$$

Considering that $\varepsilon << 1$, $1/1 + \varepsilon$ can be approximated with $1 - \varepsilon$, and hence {15} can be written as

$$\frac{d}{dt}\int_{x_{i-1}(t)}^{x_i(t)} (1-\varepsilon_x(x,t)) dx = v_{i-1}(1-\varepsilon_{x_{i-1}}(x,t)) - v_i(1-\varepsilon_{x_i}(x,t)) \quad \{16\}$$

Using the Leibnitz rule for the differentiation of integrals:

$$\frac{d}{dt}\int_{\phi(t)}^{\psi(t)} f(x,t)dx = \int_{\phi(t)}^{\psi(t)} \frac{\partial f(x,t)}{\partial t} dx + \frac{d\psi}{dt} f(\psi(t),t) - \frac{d\phi}{dt} f(\phi(t),t) \quad \{17\}$$

and assuming uniform strain throughout the span, {16} can be expressed as

$$-\frac{d\varepsilon_{x_i}}{dt}(x_i - x_{i-1}) + (1-\varepsilon_{x_i})\frac{dx_i}{dt} - (1-\varepsilon_{x_{i-1}})\frac{dx_{i-1}}{dt} = v_{i-1}(1-\varepsilon_{x_{i-1}}) - v_i(1-\varepsilon_{x_i}) \quad \{18\}$$

Simplifying {18} gives the following dynamic equation for strain in the *i*-th span:

$$\frac{d\varepsilon_{x_i}}{dt} = \frac{v_i(1-\varepsilon_{x_i}) - v_{i-1}(1-\varepsilon_{x_{i-1}}) + (1-\varepsilon_{x_i})\dot{x}_i - (1-\varepsilon_{x_{i-1}})\dot{x}_{i-1}}{x_i - x_{i-1}} \qquad \{19\}$$

Depending on the property of the web it is possible to introduce a constitutive relationship between strain and tension. Assuming the web to be elastic, Hooke's law ($T = EA\varepsilon$) can be used to describe this relationship. Substituting Hooke's law in {19} and simplifying, the following dynamic equation for the tension in the span is obtained:

$$\dot{T}_i = \frac{v_i(EA - T_i) - v_{i-1}(EA - T_{i-1}) + (EA - T_i)\dot{x}_i - (EA - T_{i-1})\dot{x}_{i-1}}{x_i - x_{i-1}} \qquad \{20\}$$

This equation includes the hypothesis that both the end rollers are free to move (that is, the control volume boundaries are time-varying).

The basic model considers the case where both rollers are stationary; in this situation Equation {20} is given by

$$\begin{aligned} \dot{T}_i(t) &= \frac{v_i(t)(EA - T_i(t)) - v_{i-1}(t)(EA - T_{i-1}(t))}{L} \\ &= \frac{EA}{L}(v_i(t) - v_{i-1}(t)) + \frac{1}{L}[v_{i-1}(t)T_{i-1}(t) - v_i(t)T_i(t)] \end{aligned} \qquad \{21\}$$

Idle and Driven Roller Models

Figure 3 shows a schematic of a driven roller (for an idle roller set $\tau_i = 0$). The dynamic equation is obtained by using torque balance. The equation for a driven roller is

$$J_i\dot{\omega}_i = -b_i\omega_i + R_i(T_{i+1} - T_i) + \tau_i \qquad \{22\}$$

where τi is the driving torque at the roller shaft, J_i is the inertia of the roller, ω_i is the angular velocity, bi is the viscous friction coefficient, and R_i is the radius of the roller.

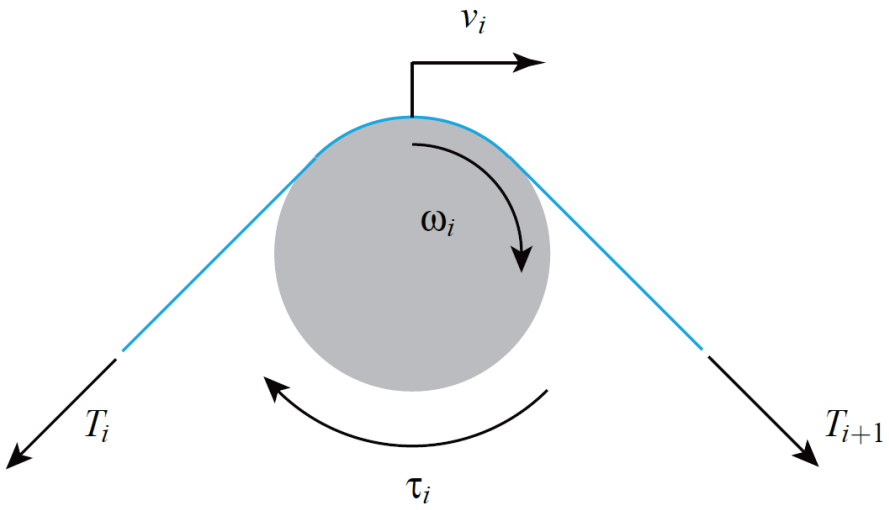

Figure 3 – Driven Roller

NONLINEAR SYSTEM IDENTIFICATION AND MODEL VALIDATION

Model validation aims to give a qualitative or quantitative measure of how well a simulated model matches a real system. Model validation can be considered as the final step of the system identification process. System identification is the procedure through which a set of equations called the model is generated starting from a combination of physical insight and experimental data; the model is expected to reproduce the behavior of the real system.

In a general sense, system identification can be divided into the following phases:

- Model order: determine the number of input, output and state variables.
- Model structure: define the relations between the input, output and state variable variables.
- Parameter evaluation: find the best parameters for the chosen model.
- Model validation: test phase that guarantees the correctness of modeling and/or identification procedure.

Nonlinear system identification and validation presents a much bigger challenge over linear system identification for several reasons. First, the structure of linear systems is simpler and the use of frequency domain analysis is possible which makes the identification process easier. Second, using the superposition property of linear systems and the property of white noise, it is possible to cover the effect of all the possible inputs just using zero mean white noise as input to the system. And finally, during the validation step, it is possible to extrapolate information about the corrections that should be made to the model through a statistical analysis of the difference between the estimated model data and real data. These statements do not hold in the case of nonlinear systems. In fact, the possible structures of nonlinear systems differ widely and achievable results strongly depend on the choice of the model structure. The performance of the model can be guaranteed only for a set of inputs used during the identification and/or validation process, in other words the ability of the model to match the output due to unseen inputs

is uncertain. Also, the validation step does not in general give insights into modifications of the model when the test used to compare model and experimental data does not pass. The rest of the section will cover a brief overview of existing nonlinear system identification techniques and some validation procedures.

Nonlinear System Identification

Nonlinear system identification can be achieved through several different techniques based on the problem at hand. A classification of the different techniques can be made based on the amount of a priori information available about the system. Based on this concept, the identification techniques can be classified into the following:

- Black box identification: applied when prior knowledge of the system is not available. This is used in situations where only input/output data are available to describe the system, and a model that is capable of matching this input/output data needs to be found.
- Grey box identification: applied when some prior knowledge of the system is available. This is used when most of the dynamics and parameters of the system can be determined from first principles, but still some effects are not known and system identification is left to some sort of input/output data matching.
- White box identification: it is adopted when there is total knowledge about the system and all the dynamics and the parameters can be deduced without experimental data.

Clearly, it is desirable to exploit prior information about the system as much as possible. Therefore, as a general idea it is preferable to move toward the bottom of the above classification list when possible. However undesirable, often the only choice for identification is the black box approach and, for this reason, there is a rich literature concerning strategies to perform this kind of identification, see [4] for a detailed survey. In a general sense, the problem faced during black-box identification is the following: given two sets of recorded data

$$\mathbf{u}^t = [u(1), u(2), \ldots, u(t)] \qquad \mathbf{y}^t = [y(1), y(2), \ldots, y(t)] \qquad \{23\}$$

the input and the output, respectively, of a certain system, find the function:

$$\hat{y}(t) = g(\mathbf{u}^{t-1}, \mathbf{y}^{t-1}) + v(t)$$

which gives the best match between the recorded data $y(t)$ and the estimated data $\hat{y}(t)$ while keeping the additive term $v(t)$ as small as possible.

For black box system identification, validation is done by testing the performance of The model on a set of input/output data not used during the parameter estimation step. This set is, therefore, called the validation data. If the model gives satisfactory performance on the validation data, then the model is accepted. Otherwise it is necessary to go back and restart the process of testing different structures for the model.

Even though there is a well-established theory about nonlinear system identification, it does not fit the purpose of model validation that is sought in the web line case. Using a black box model for web handling would mean discarding all the knowledge about the dynamic behavior of the web and other primitive elements obtained using first principles approach.

Some gray box techniques have been developed in order to exploit prior knowledge about the system in the identification process; examples are given in [5] where the concept of semi-physical modeling is introduced, and in [6] where a priori physical knowledge is introduced in a neural network framework. The goal of these techniques is to combine strategies from black-box approaches with equations derived from physical reasoning.

As reported in [5], in order for this procedure to be applicable the model must satisfy certain requirements. Moreover, the size of the model could make the procedure computationally untractable. Unfortunately, due to the presence of non-smooth nonlinearties and because of the high complexity of web handling machines this procedure is not applicable.

Since none of the identifications techniques found in the literature can be adapted to the model that has been developed for the web machines, validation techniques that are appropriate variations of white-box modeling will be discussed next.

Model Validation

When a model is developed using physical laws like conservation of mass or energy, a *general model* is obtained. This general model should be able to describe all the systems belonging to the same class just by adjusting the parameters of the model. For example, it is expected that the general model developed for the web line is able to describe any web line just by adding the right amount of primitive elements with the right parameters. If the parameters in a general model are fixed, the resulting model is called the *specific model*. The model for the EWL is a specific model of a web machine. Finally, once initial conditions and both forcing and disturbance inputs are added to the model, the *particular model* is obtained. The model validation process is to infer the correctness of the general model by means of a variety of specific models. Clearly, this process does not guarantee that the general model is exact unless every possible particular model is tested for each specific model, which is practically unrealizable [7]. Normal practice is to define a set of relevant experiments to test the model and validate the model if the performance on this set is satisfactory. The measurement of performance of the model is another key aspect of the validation process and it is difficult to define a criterion which fits all the possible scenarios. The easiest choice to judge the performance of the model is through a visual comparison of the output signals as a function of time. In this case experimental data is plotted with simulated data and it is left to the user to judge whether the model is acceptable or not. The performance can also be weighted based on selection of a norm, the most commonly used norms are L_1 (the integral of the absolute value of the error), $L2$ (the integral of the squared error) or L_∞ (the maximum error); in this case the fitting error would be used as a testing parameter and the model is required to satisfy a preset bound on the chosen norm. The norm of the fitting error can also be a good parameter to judge between different models as well. Note that this does not give an absolute criterion, in fact it is possible to have a model outperforming another one based on a certain norm.

In order to have a validation test which depends less on the choices made by the user, the *model distortion* technique was introduced in [8, 9]. The concept behind the model distortion is that any set of recorded data can be followed by any model if the model is distorted using time varying parameters. Clearly, if the model matches the real system closely, less parameter variation is required in order to make the simulated data follow the recorded data. From this observation a quantitative criterion for model validation arises. In fact, since the model is derived fromsome physical understanding of the process, every parameter has a physical meaning, and hence, it is reasonable to assume that for every parameter an estimation of its variance is available. Therefore, if parameter distortion necessary to have a perfect match between simulation and experimental data has variance

less than the expected one, then it is possible to claim that the model is able to explain. Otherwise, the model needs to be modified. Note that the model distortion technique is just a pass or fail criterion and does not give any insights into how the model should be adjusted to better follow experimental data. This framework gives a more structured test for model validation compared to the simple visual comparison. However, reasonable bounds on the variance of the parameters are seldom available. In such situations the choice of the bound and, implicitly, the acceptance or rejection of model falls on the user, and the model distortion approach does not give any real advantage over visual comparison. In certain situations model distortion can still be a useful tool to perform sensitivity analysis to parameter variations.

Based on the literature review, most of the model validation techniques rely on visual comparison over a set of experiments of interest, and beside the model distortion approach there is not a well-established theory to achieve model validation for nonlinear systems. Hence, model validation for the EWL will be approached based on FFT analysis and visual comparison between simulated and experimental data on a set of experiments which cover the most common situations in web lines.

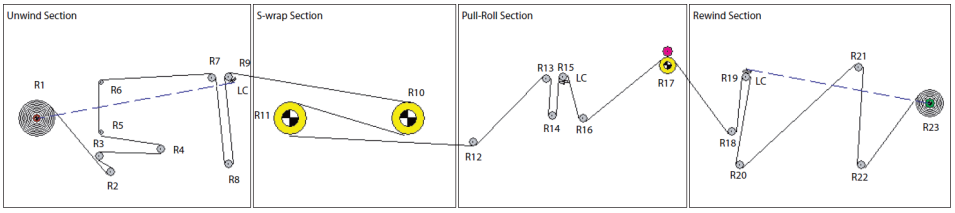

Figure 4 – The Euclid Web Line (EWL).

EXPERIMENTAL VALIDATION AND MODEL MODIFICATIONS

Experimental Setup

Normally, when performing validation of a model, experiments are performed in an open loop setup. Unfortunately, it is not possible to run web machines in open-loop because even a small disturbance can induce large tension variations which may cause web breakage. Another possibility is to run experiments in a hardware in the loop configuration, which is to run the experiments in closed-loop, recording the control input, and using that input as model input. Initially, the hardware in the loop configuration was tested, but this did not give satisfactory results. There are two plausible reasons for this. First, in the real control input there are adjustments for disturbances which are not modeled. Second, the control input that can be recorded is not the actual input to the motor but it is a reference for the controller that drives the AC motor. Therefore, the real input to the web machine may differ from the one recorded. For these reasons a closed-loop setup was chosen to run the experiments, meaning that the simulation of the system would also include a model of the controller. In this configuration the inputs for the model are reference values of tensions and web velocity.

All of the experimental data presented in this report has been collected on the Euclid Web Line (EWL). The web line can be divided into four sections: the unwind section, the S-wrap section, the pull-roll section, and the rewind section. The S-wrap functions as the master speed section. The S-wrap and pull-roll are under pure speed control, whereas the unwind and rewind have an inner speed loop and an outer tension loop. Hence, tension is regulated in the unwind and rewind sections only.

The EWL offers the possibility of choosing different web paths with different span lengths and number of idle rollers. The configuration used to perform all the experiments is shown in Fig. 4. Roller number 9 is mounted on load cells which measure the tension for the unwind section and provides the feedback signal for the unwind tension PI controller. The roller 15 is also mounted on load cells and it gives the tension in the pullroll section which is only used for monitoring purposes. Tension is measured on roller 19 in the rewind section. All the experimental data discussed in this paper correspond to the unwind section of the EWL.

All the velocity controllers are of the form:

$$C_v(s) = \frac{K_p(s+\omega_{ld})}{s} \qquad \{24\}$$

where $K_p = JK_{ref}$, with J as the total inertia reflected at the motor side, $\omega_{ld} = K_{ref}/4\zeta^2$, where $\zeta = 1.1$ is the damping ratio. The values of K_{ref} for unwind, S-wrap leader, S-wrap follower, pull-roll and rewind, respectively, are 15, 20, 20, 40 and 15.

The tension PI for the unwind and rewind are

$$C_t^{unw}(s) = \frac{2(s+10)}{2} \qquad C_t^{rew}(s) = \frac{3(s+10)}{2} \qquad \{25\}$$

A model of the full line based on the dynamic equations described earlier and a model of all the controllers has been implemented in Simulink. The entire line is simulated for all cases but only the data from the unwind section will be shown for comparison with the experimental data.

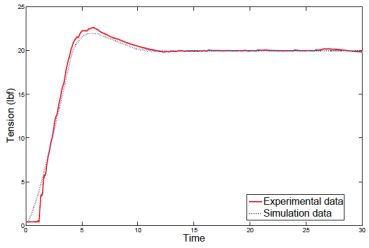

(a) Experimental and simulated data comparison for a step reference change of 20 lbf with zero line speed.

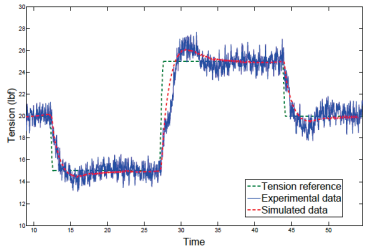

(b) Comparison of experimental and simulated data for step reference changes with non-zero line speed.

Figure 5 – Results from Basic Primitive Element Simulation.

Results from Basic Primitive Element Model Simulations and Experiments

The initial set of experiments consisted of a step change in tension reference with zero line speed. The purpose of these experiments was to verify if the model is capable of reproducing tension behavior when speed induced disturbances are not present. Different reference values were tested with different gains for the tension PI. The result for a step in tension of 20 lbf is shown in Fig. 5(a). All the experiments showed that the model simulated data can follow the experimental data closely.

The second set of experiments considered also a step change in tension reference, but with a non-zero line speed. In this case, speed induced disturbances are observed in the

tension signal and it is necessary to verify if the model is able to reproduce these speed induced disturbances. For this case different step changes and different PI gains were tried. Data from one of the experiments is shown in Fig. 5(b). In general, the model simulated data appears to be able to follow the average value of the tension but does not reproduce the speed induced oscillations. From these preliminary experiments the need for modifications to the existing model to capture the speed induced disturbances is clear.

Effect of Out-of-Round Material Roll

For an out-of-round material roll, when the roll rotates the release point of the material changes with time. This implies that the length of the first web span between the material roll and the first idle roller changes as well. Therefore, the dynamic equation for the web span with constant span length {21} cannot be used. It is necessary then to use the general equation for the web span given by {20}. Since the first idle roller is stationary, {20} can be simplified by defining $L(t) = x_i(t) - x_{i\text{-}1}(t)$:

$$\dot{T}_i(t) = \frac{v_i(t)(EA - T_i(t)) - v_{i-1}(t)(EA - T_{i-1}(t)) + (EA - T_i(t))\dot{L}(t)}{L(t)} \qquad \{26\}$$

To simulate the tension dynamics for such a situation it would be necessary to determine an expression for $\dot{L}$. Given a generic shape for the roll, finding an analytical expression for $\dot{L}$ may not possible in general; details on how to numerically compute an expression for $L(t)$ can be found in the companion paper [10].

Once the numerical value of $L(t)$ is available at each time instant, a numerical approximation for $\dot{L}(t)$ can be obtained and used in the simulation of web tension dynamics. Independent of the shape of the roll, the function $L(t)$ will repeat itself after each revolution of the roll (ignoring change in radius). The span length $L(t)$ is periodic with period $T = 2\pi/\omega$ where w is the angular velocity of the roller. Every periodic function $g(t)$ of frequency f can be expanded in a Fourier series with the fundamental frequency equal to f:

$$g(t) = \sum_{j=1}^{\infty} C_j \sin(2\pi j f t + \psi_j) \qquad \{27\}$$

Therefore, $L(t)$ can be written as

$$L(t) = \sum_{j=1}^{\infty} C_j \sin(2\pi j f t + \psi_j) \qquad \{28\}$$

where $f = \omega/2\pi$, and hence

$$\dot{L}(t) = \sum_{j=1}^{\infty} 2\pi j f C_j \cos(2\pi j f t + \psi_j) \qquad \{29\}$$

Since the tension dynamics {26} is a function of $L(t)$ and $\dot{L}(t)$, the length change in the span introduces disturbances of frequencies f, $2f$, $3f$, . . . in web tension. This was also verified experimentally on the Euclid web line. Given the web line velocity v [FPM] and the radius R [in] of the unwind roll, the angular velocity of the roll is given by

$$\omega = \frac{v}{5R}\left[\frac{rad}{s}\right] \quad \{30\}$$

and the corresponding fundamental frequency is

$$f = \frac{\omega}{2\pi} \quad \{31\}$$

Figure 6(a) shows the FFT of tension corresponding to a web velocity of 200 FPM and unwind radius of 6.375 in; these values correspond to f = 0.97 Hz. It is clear from Fig. 6(a) that the tension signal contains frequencies f, $2f$, $3f$, and so on. To further consolidate the claim that the oscillations are due to out-of-roundness of the material roll, other velocities have been tested. The values of the fundamental frequency computed through equations {30} and {31} at 100 FPM, 200 FPM and 300 FPM, respectively, are 0.485 Hz, 0.97 Hz and 1.455 Hz. Figure 6(b) shows the first peak of the FFT of the data at different velocities. Results show a match between the computed values and the experimental data.

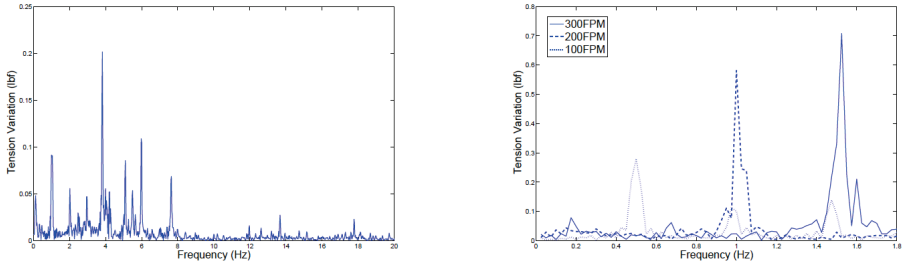

(a) Experimental data; line speed=200 FPM, unwind radius=6.375 in

(b) First peak with different web velocities

Figure 6 – Frequency content of the tension data

To reproduce the effect of the out-of-round unwind roll in model simulations, instead of computing $\dot{L}$ from the shape of the roller, it was chosen to approximate the function with the first six terms of the Fourier series:

$$\dot{L}(t) = \sum_{j=1}^{6} 2\pi j f C_j \cos(2\pi j f t) \quad \{32\}$$

Figure 7 shows the results from the model simulation and the experiment. With the inclusion of the effect of the out-of-round roll in the model, the frequency content of the data from simulations is much closer to the frequency content of the experimental data. This indicates that the effect of the out-of-round roll cannot be neglected in the model.

Experiments with Out-of-Round Material Roll

To amplify the effect of out-of-round material roll, some experiments were conducted with the unwind roll made purposely out-of-round; a bump was introduced into the unwind roll by placing a solid metal shaft in the middle of the material and winding material over it. The result of the experiment with line speed of 200 FPM is shown in

Fig. 8. It can be observed that the out-of-roundness of the roll deteriorates the tension signal further than what was observed before. It should be noted that, as expected, since only the shape of the roller changed, and not its angular velocity, the frequency content of the tension signal did not change when compared with the one obtained from the normal roll (see Fig. 6(a)); the changes are simply in the amplitude of the disturbance at every frequency. Moreover, the fundamental frequency $f = 0.97$Hz and its multiples are clearly visible.

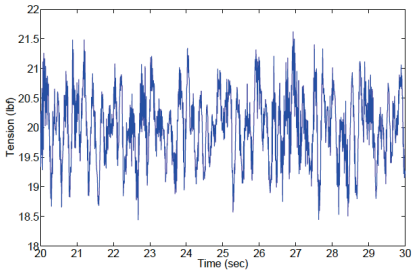

(a) Experimental data (time domain)

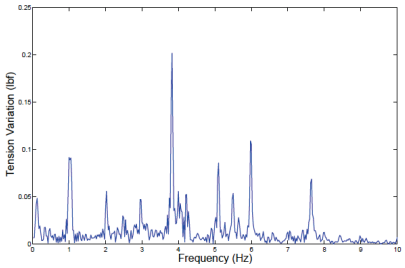

(b) Experimental data (frequency domain)

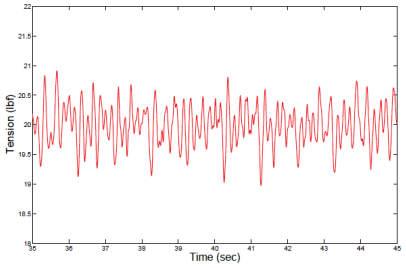

(c) Model simulated data (time domain)

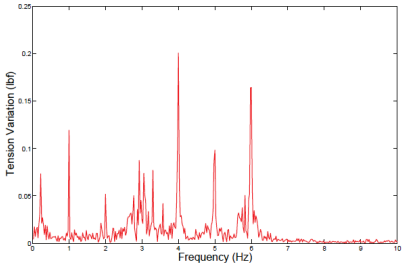

(d) Model simulated data (frequency domain)

Figure 7 – Comparison of experimental and model simulation data at 200 FPM

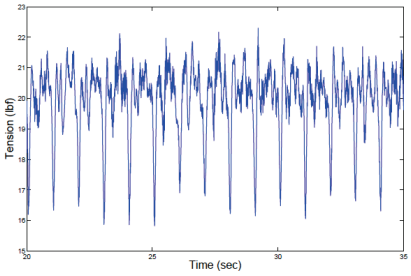

(a) Experimental data (time domain)

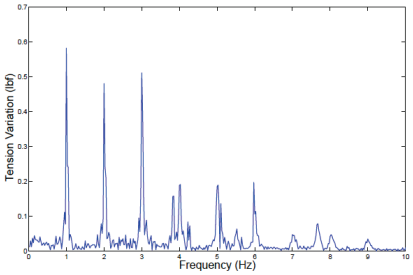

(b) Experimental data (frequency domain)

Figure 8 – Experiments results with out-of-round material roll (line speed=200 FPM)

Disturbances in Tension That Are Not Due to the Out-of-Round Material Roll

Another set of experiments was performed to identify which frequencies in the frequency spectrum are not due to the out-of-round material roll. From {30} and {31} it

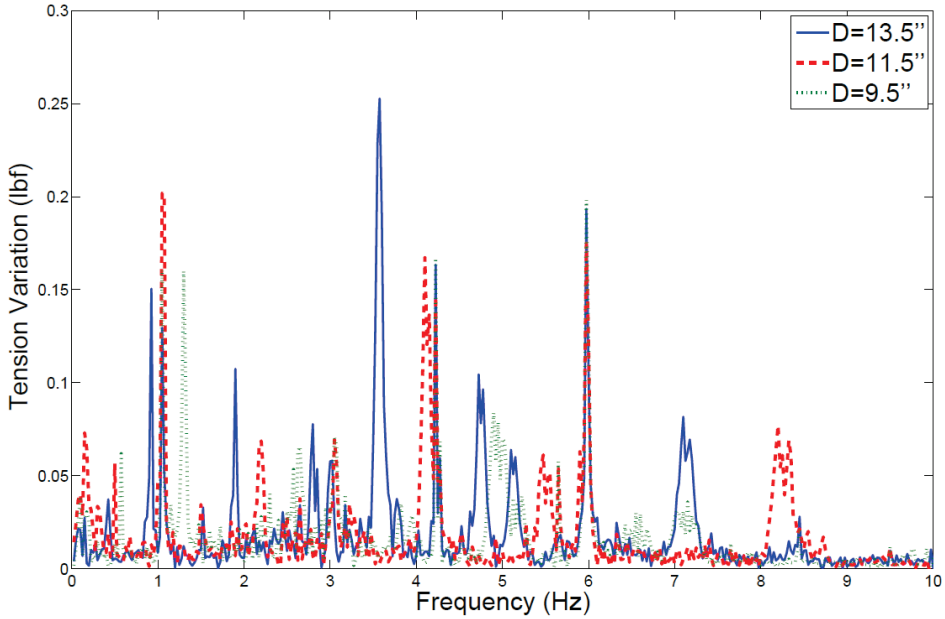

Figure 9 – Experimental data with material roll at different radii (line speed = 200 FPM)

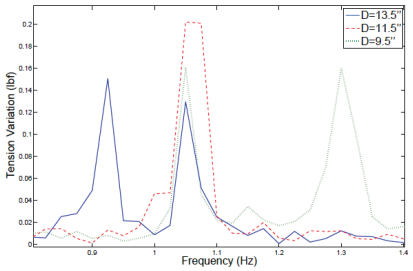

(a) First peak due to out-of-round material roll

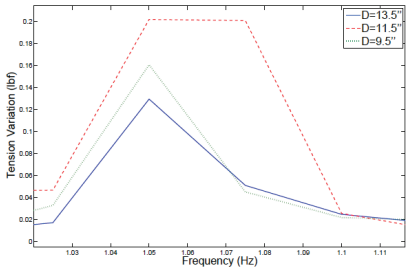

(b) Zoom around $f_1 = 1.05$ Hz

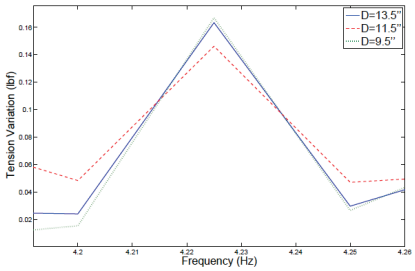

(c) Zoom around $f_2 = 4.23$ Hz

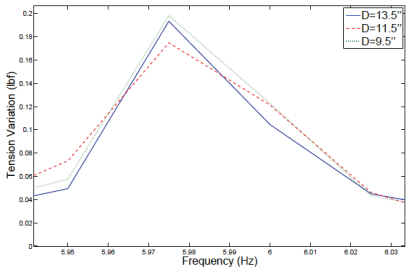

(d) Zoom around $f_3 = 5.97$ Hz

Figure 10 – Detailed views around select frequencies (line speed = 200 FPM)

can be noted that the fundamental frequency of the disturbances due to the out-of-round material roll depends on the radius of the material roll. This can be exploited to isolate the frequencies which are not due to the out-of-round material. Experiments were conducted at 200 FPM with different values for the radius of the material roll. The results are plotted in Fig. 9. Additional insights can be drawn from these experiments. First, it can be observed that the fundamental disturbance frequency due to the out-of-round material roll changes when the radius changes. Note that for radius values of $R_a = 6.75$ in, $R_b = 5.75$ in and $R_c = 4.75$ in, the corresponding fundamental disturbance frequencies due to the out-of-round material roll are $f_a = 0.94$ Hz, $f_b = 1.11$ Hz and $f_c = 1.34$ Hz, which can be clearly seen in Fig. 10(a). One can also observe the presence of three different disturbances and their multiples that are not affected by the change in unwind roll radius, in particular the values $f_1 = 1.05$ Hz (see Fig. 10(b)), $f_2 = 4.23$ Hz (see Fig. 10(c)), and $f_3 = 5.98$ Hz (see Fig. 10(d)). Now assuming that these disturbances are induced by rotating elements, using {30} and {31} it is possible to determine the radius of the rotating elements causing these disturbances. The radii corresponding to these fixed frequencies are

$$R_1 = \frac{v}{2\pi f_1} = 6.05 \text{ in}, \quad R_2 = \frac{v}{2\pi f_2} = 1.5 \text{ in}, \quad R_3 = \frac{v}{2\pi f_3} = 1.1 \text{ in} \qquad \{33\}$$

These three radii, respectively, are the radius of the S-wrap lead roller, idle rollers, and the web guide rollers.

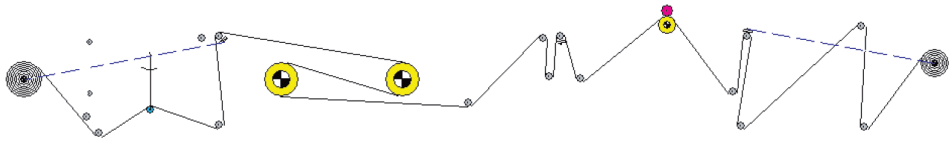

(a) Alternative web path excluding the guide rollers

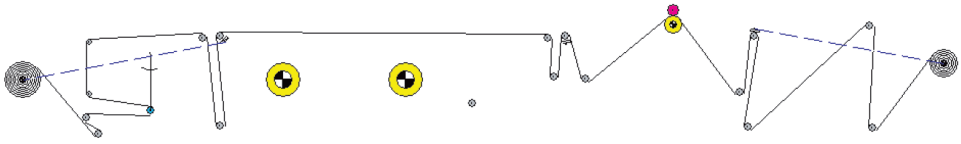

(b) Alternative web path excluding the S-wrap rollers

Figure 11 – Schematics for the alternative paths.

To further verify these observations, experiments were conducted with two different web paths: one excluding the web guide and the other excluding the S-wrap. Fig. 11 shows the schematics of the two web paths. The results of the experiments are shown in Fig. 12. Fig. 12(b) shows how the 1.1 Hz disturbance is present in the tension FFT obtained using the regular path and is absent in the tension FFT with the path excluding the S-wrap. This shows how the eccentricity or out-of-roundness of the S-wrap is indeed responsible for the presence of the 1.1 Hz disturbance. Figure 12(a) shows that the 6 Hz signal for the web path with no guide is much smaller in compared to its value in the FFT of the regular path. Also, from Fig. 12(b) it can be observed that the 6 Hz signal

completely disappears in the tension FFT with no S-wrap, which indicates that this is due to the S-wrap.

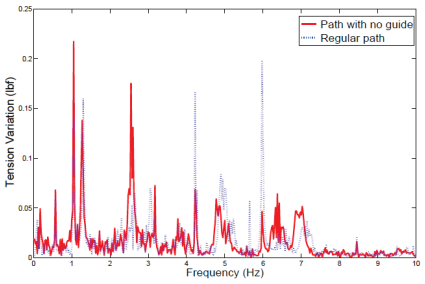

(a) Tension signal for web path of Fig. 11(a)

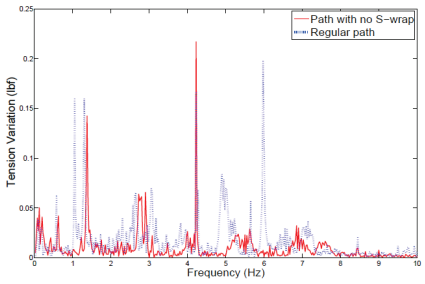

(b) Tension signal for web path of Fig. 11(b)

Figure 12 – Tension signal FFT for the regular web path and alternative web paths

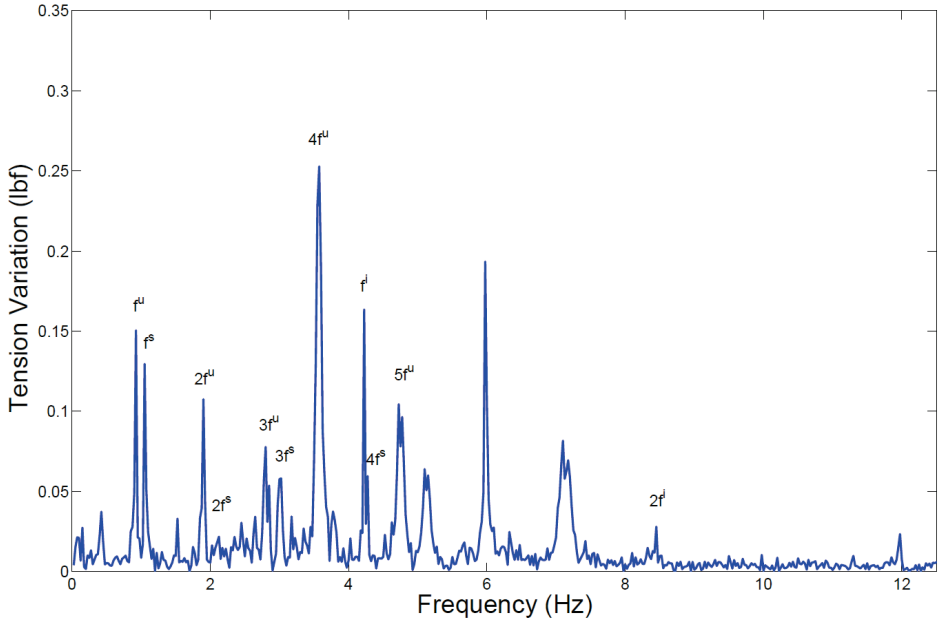

Figure 13 – Tension signal FFT for unwind roll diameter D = 13.5 in with line speed of 200 FPM. Every peak can be identified as a multiple of one of the fundamental frequencies, f^u fundamental frequency due to unwind roll, f^s fundamental frequency due to S-wrap, f^i fundamental frequency due to idle rollers.

From this analysis, it is now possible to identify the source of most of the frequency components in the tension signal. From the above discussion, every non-ideal element will introduce oscillations in tension. These oscillations contain frequencies that are integer multiples of the fundamental frequency that can be calculated for each element knowing its radius and the line speed. As an example, consider Fig. 13 which shows the tension FFT with the unwind diameter of 13.5 in and line speed of 200 FPM. For this configuration, the fundamental frequency of the disturbances due to out-of-round material

roll is f^u = 0.95 Hz, the one due to the S-wrap is f^s = 1.05 Hz, and the one due to idle rollers is f^i = 4.23 Hz. Figure 13 shows how it is possible to tag most of the peaks in the tension FFT as being caused by the effects discussed above.

CONCLUSIONS

The paper described efforts to validate tension dynamic models. A large experimental platform called the Euclid Web Line was used to validate the models. A computer simulation of the EuclidWeb Line based on the primitive element models was developed to compare the experimental data with the data generated by simulation of the theoretical models.

Simulations with existing models showed that these models were able to follow the experimental data in an average sense, but they were not able to reproduce the oscillations around the average value which were seen in the experimental data. Therefore, model improvements were necessary to capture the experimental data. It was found that an out-of-round material roll produces length variations in the web span adjacent. The mechanism that incorporates the effect of out-of-round rolls and eccentric rollers into the tension model is the inclusion of length variations. The tension model that includes span length variations due to out-of-round rolls or eccentric rollers is able to closely predict experimental data.

ACKNOWLEDGMENTS

This work was supported by the Web Handling Research Center, Oklahoma State University, Stillwater.

REFERENCES

1. Pagilla, P. R., Siraskar, N. B., and Dwivedula, R. V., "Decentralized Control of Web Processing Lines," IEEE Transactions on Control Systems Technology, Vol. 15, January 2007, pp. 106–116.
2. Branderburg, G., "New Mathematical Model for Web Tension and Register Error," in Proceedings of the 3rd International IFAC Conference Instrumentation Automation Paper, Rubber Plastic Industry, 1977, pp. 411–438.
3. Shelton, J. J., "Dynamic of Web Tension Control with Velocity or Torque," in Proceedings of the American Control Conference, 1986, pp. 1423–1427.
4. Sjöberg, J., Zhang, Q., Ljung, L., Benveniste, A., Delyon, B., Glorenned, P. Y., Hjalmarsson, H., and Juditsky, A., "Nonlinear Black-Box Modeling in System Identification: a Unified Overview," Automatica, Vol. 31, no. 12, 1995, pp. 1691–1724.
5. Lindskog, P. and Ljung, L., "Tools for Semiphysical Modeling," International Journal of Adaptive Control and Signal Processing, Vol. 9, Nov. 1995, pp. 509–523.
6. Oussar, Y. and Dreyfus, G., "How to be a Gray Box: Dynamic Semi-Physical Modeling," Neural Networks, Vol. 14, No. 9, 2001, pp. 1161–1172.
7. Thomas, P., Simulation of Industrial Process for Control Engineers. Oxford, UK: Butterworth and Heinemann, 1999.
8. Butterfield, M. H. and Thomas, P. J., "Methods of Qualitative Validation for Dynamic Simulation Model - Part 1: Theory," Transactions of the Institute of Measurement and Control, Vol. 8, 1986, pp. 182–200.

9. Cameron, R. G., “Model Validation by the Distortion Method: Linear State Space,” IEE Proceedings-D, Vol. 139, May 1992, pp. 296–300.
10. Branca, C., Pagilla, P. R., and Reid, K. N., “Computation of Span Length Variations Due to Non-Ideal Rolls,” Proceedings of the Tenth Intl. Web Handling Conference, 2009.

Name & Affiliation	**Question**
Unknown	In your experimental results, it appears all the frequencies are due to some kind of excitation or disturbances. Can you explain that? How do they affect the system?
Name & Affiliation	**Answer**
C. Branca, Oklahoma State University	We have purposefully made the unwind roll out-of-round to introduce web tension oscillations or disturbances. The out-of-round unwind roll, and other eccentric rollers within the web line, produce tension oscillations of different frequencies and amplitudes. We think that the tension oscillation of the largest amplitude is closer to a system resonant frequency. The tension oscillations are reflected in the model through length variations that are caused by the out-of-round roll.
Name & Affiliation	**Question**
Tim Walker, T. J. Walker & Associates	When you made your wound roll out of round, how severely out of round did you make it? If you fueled the out-of-roundness of the rollers, would that give you the upset? What was the web you did these experiments on?
Name & Affiliation	**Answer**
C. Branca, Oklahoma State University	A half-inch diameter rod with length slightly larger than the width of the web was introduced in the middle of the material roll and the web was subsequently wound onto it to produce an out-of-round shape for the roll which looked elliptical. The web material was Tyvek.
Name & Affiliation	**Question**
Tim Walker, T. J. Walker & Associates	How far out-of-round were your rollers?
Name & Affiliation	**Answer**
C. Branca, Oklahoma State University	We were not able to quantify the out-of-roundness of the rollers on the line. There appears to some amount of eccentricity in the idle rollers and one of the S-wrap rollers.
Name & Affiliation	**Question**
Tim Walker, T. J. Walker & Associates	You are measuring all of this at one position using one load cell roller. Would you imagine the upsets would be different depending upon which span you were looking at? A continuation of high frequency tension upsets occurs as you pass through rollers; it doesn't necessarily transmit 100% from one span to another.
Name & Affiliation	**Answer**
C. Branca, Oklahoma State University	Yes, the tension oscillations would be different as one looks at the downstream spans from the source of disturbance; they would actually decrease.
Name & Affiliation	**Question**
Tim Walker, T. J.	You have two different web paths. In one path you have 6-7 rollers between the unwind roll and the tension roll. In the

	other web path, I don't know how schematically correct it is, there are no rollers between the unwinding roll and the load cell roller. Did you see a big upset from your unwinding roll and the different web paths? What was the magnitude of the tension change?
Name & Affiliation	**Answer**
C. Branca, Oklahoma State University	In one web path there were five idle rollers from the unwind roll to the roller containing the load cells and in the other we have only one idle roller between the unwind roll and the load-cell roller. The frequency content and amplitude of oscillations in the tension signal are different for the two web paths due to different number of idle rollers between the unwind roll and the load-cell roller, although several similar dominant frequencies are found in both web paths which may be due to the out-of-round unwind roll.